

Physical Properties of Carbon Nanografibers

Y. Ando*, X. Zhao**, H. Kataura***, Y. Achiba***, K. Kaneto****,
S. Uemura***** and S. Iijima*¹, ***, *****

*Dept. of Physics, Meijo Univ., Tempaku-ku, Nagoya 468-8502, Japan

Fax: 81-52-832-1170, e-mail: yando@meijo-u.ac.jp, iijimas@meijo-u.ac.jp

**JST-ICORP, c/o Dept. of Physics, Meijo Univ., Tempaku-ku, Nagoya 468-8502, Japan

Fax: 81-52-834-4001, e-mail: zhao@meijo-u.ac.jp, iijimas@meijo-u.ac.jp

***Tokyo Metro. Univ., Hachioji, Tokyo 192-0397, Japan

Fax: 81-426-77-2483, e-mail: kataura@phys.metro-u.ac.jp, achiba-yohji@c.metro-u.ac.jp

****Kyushu Inst. Technol., Iizuka, Fukuoka 820-8502, Japan

Fax: 81-948-29-7651, e-mail: kaneto@pisces10.cse.kyutech.ac.jp

*****Ise Electronics Corp., Ise 516-1103, Japan

Fax: 81-596-39-0665, e-mail: SGX03334@nifty.ne.jp

*****NEC Corp., Tsukuba, Ibaraki 305-8501, Japan

Fax: 81-298-56-6136, e-mail: s-ijima@frl.cl.nec.co.jp

High-quality multiwalled carbon nanotubes (nanografibers) with high graphitization and very narrow central channel were prepared by DC arc discharge in rarefied pure hydrogen gas. Because such nanografibers coexisted with few carbon nanoparticles, they could be easily purified by exposing infrared radiation in air. Raman spectra of aligned nanografibers showed typical Raman-allowed phonon mode, E_{2g} , of graphite at near 1580cm^{-1} and a new peak at near 1850cm^{-1} . The electrical conductivity measurements of individual purified nanografibers indicated that they could conduct an enormalous current density of more than $10^7\text{A}/\text{cm}^2$. High yield of nanografibers was attained by automatic control of the feed of the cathode.

Key words: nanografiber, carbon, Raman spectra, electrical conductivity

1. INTRODUCTION

Multiwalled carbon nanotubes were first found by one [1] of the present authors, in the cathode deposit obtained by DC arc discharge evaporation of pure graphite rods in helium gas. When the evaporation has been carried out in rarefied pure hydrogen gas [2,3], high-quality multiwalled carbon nanotubes with high graphitization and very narrow central channel could be obtained. Their high-quality multiwalled carbon nanotubes prepared in hydrogen gas were named as "nanografibers" [4]. Because such nanografibers coexisted with few carbon nanoparticles, they could be easily removed by the irradiation of infrared radiation in air [5]. Namely, nanografibers were entirely purified.

In the present study, pristine and purified nanografibers were observed by using a high resolution SEM (scanning electron microscopy). Some aligned nanografibers were obtained by pressing the specimen surface with a spatula. Micro Raman spectra of aligned nanografibers were measured by non-polarized and polarized incident laser beam with various powers. Measurements of electrical resistivity and its temperature dependency for nanografibers were done. Field emission measurements for purified nanografibers also were carried out.

Mass production of high-quality nanografibers also is important problem. High yield of nanografibers in DC arc discharge was attained by

automatic control of the feed of the cathode. XRD (X-ray diffraction) measurements of the mass produced nanografibers were done.

2. EXPERIMENTAL

Nanografibers were obtained as a cathode deposit by evaporating pure graphite rods installed vertically in hydrogen gas of pressure $8.0 \times 10^3\text{Pa}$, by applying DC arc discharge [2,3]. DC arc current of 50A was applied through the lower anode of 6mm in diameter, and a disk-like deposit of 1mm thick was obtained on the upper cathode of 10mm in diameter after stabilized evaporation for 40sec. The central part of the cathode deposit (4 ~ 5mm diameter) includes much nanografibers and few nanoparticles. Such nanoparticles could be easily removed and nanografibers were purified by the irradiation of infrared radiation in air at 500°C for 30min [5,6].

High yield of nanografibers was attained by automatic control of the feed of the upper cathode monitoring the arc voltage as constant in hydrogen atmosphere of pressure $1.3 \times 10^4\text{Pa}$. By the evaporation of DC arc current 60A for 10min, about 1.2g in mass of cathode deposit was obtained. The deposit is covered by hard graphite shell of about 1mm thick. The inner core part (3 ~ 4mm diameter, 15mm length) of 0.15g in mass is composed of nanografibers more than 60% and remained parts are nanoparticles.

Pristine and purified nanofibers were observed by using a high resolution SEM (Topcon, ABT-150F). Micro Raman spectra using $50\times$ objective lens for aligned nanofibers were recorded by a Raman spectrometer (Jobin Yvon, RAMANOR T64000) at 514.5nm (Ar laser) [7] in various power and polarization. The electrical conductivity of individual nanofibers was measured by a two-probe method using a micro-manipulator system (Shimadzu, MMS-77), and their temperature dependency also was measured [6,8]. XRD studies of high yield nanofibers put on no-reflection silicon plate were carried out by using CuK α radiation (Shimadzu, XRD-6000).

3. EXPERIMENTAL RESULTS

3.1 SEM

A high-resolution SEM micrograph of pristine nanofibers, which was taken at the surface of the cathode deposit, is shown in Fig.1(a). Each nanofiber and their bundles can be observed as fibers. Some nanoparticles in size $15\sim 30\text{nm}$ shown by arrows in Fig.1(a) also can be seen. Because the quantity of nanoparticles are fairly few compared with the case of multiwalled carbon nanotubes prepared in helium gas [9,10], these nanoparticles can be easily removed by irradiation of infrared radiation [5,6]. Namely, nanofibers can be easily purified. An example of SEM micrographs for such purified nanofibers is shown in Fig.1(b). No nanoparticles can be observed in Fig.1(b).

Another example of SEM micrographs of nanofibers is aligned ones shown in Fig.2, in which a number of aligned nanofibers are seen. In this case, the surface of the pristine cathode deposit was pressed by using a spatula. Then nanofibers at the surface region aligned parallel with each other as seen in Fig.2 to the direction that the spatula was moved (vertically).

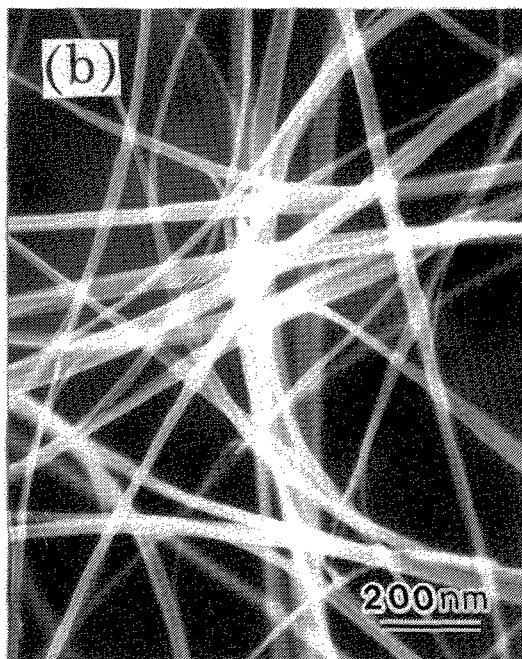
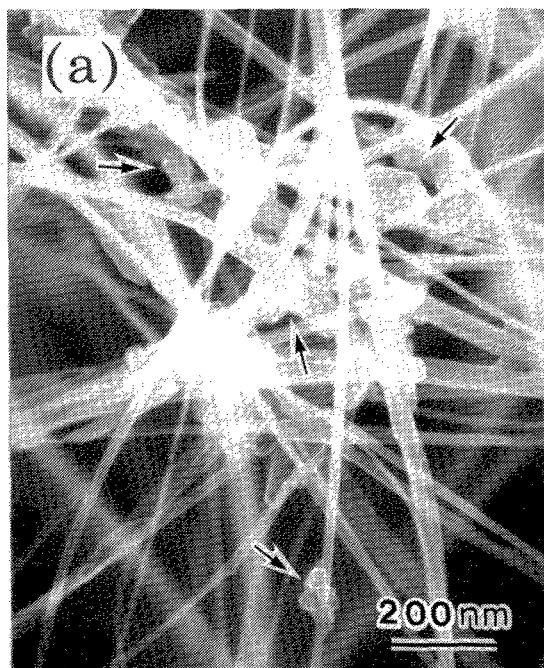


Fig.1 SEM micrographs of nanofibers. (a) Pristine and (b) purified ones.

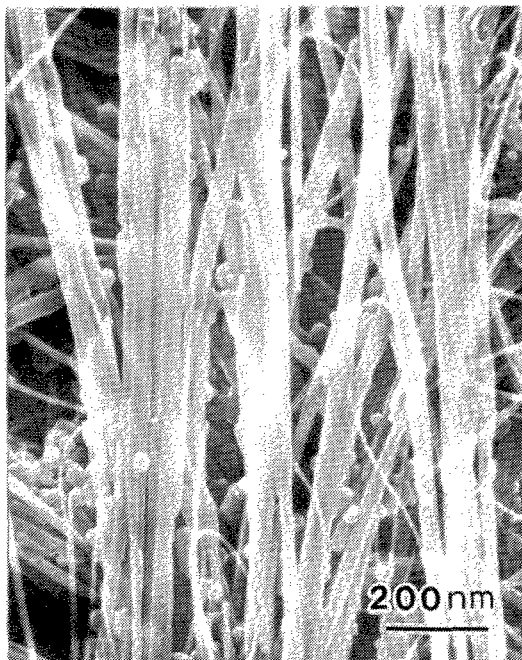


Fig.2 An SEM micrograph of aligned nanofibers.

3.2 Raman spectra

Micro Raman spectra of aligned nanofibers shown in Fig. 2 (vertically aligned) were observed by Ar laser (514.5nm) in different powers of incident beam and using polarizer. The Raman spectra of frequency range $1300\text{-}1900\text{cm}^{-1}$ are shown in Figs.3(a) and 3(b) for two incident powers 20 and 100mW, respectively.

In Figs.3(a) and 3(b), symbols P_N , P_{\perp} and P_{\parallel} mean non-polarized, vertically polarized and

parallelly polarized beam, respectively. These vertical and parallel polarization directions correspond to the direction of alignment of nanografibers. Each spectrum has strong two peaks E_{2g} and E_a , and very weak disorder peak of graphite, E_d , at near 1350cm^{-1} . The peak, E_{2g} , is known as Raman-allowed phonon mode of graphite. Other peak E_a can not be assigned by any Raman mode of graphite, namely new peak for nanografibers [7,11].

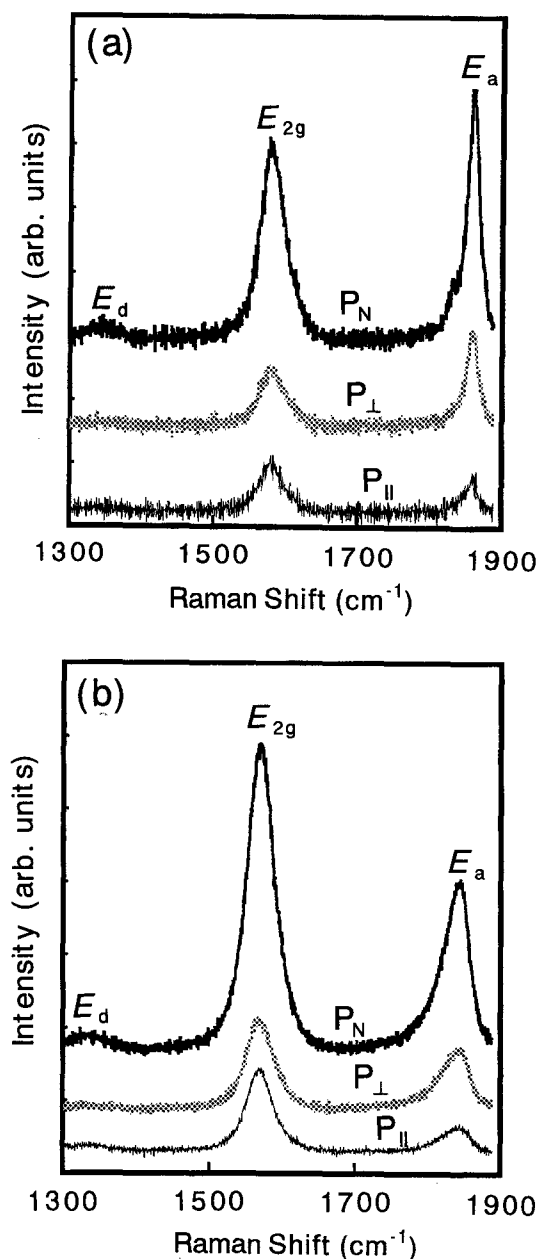


Fig.3 Raman spectra of aligned nanografibers. Incident power is (a) 20mW and (b) 100mW.

The peak positions for the two peaks, E_{2g} and E_a , shift to the low frequency side as the incident power was increased as summarized in Table I. The new peak, E_a , is double peak of very weak intensity and strong intensity for the case of low

incident power 20mW.

The new peak E_a has strong intensity than the peak of E_{2g} for the case of non-polarized and vertically polarized low incident laser power, 20mW. On the contrary, the intensity relation becomes reversely for high incident power 100mW for various polarization.

Table I Raman shift of E_{2g} and E_a for different power of incident laser beam (non-polarized)

power (mW)	E_{2g} (cm^{-1})	E_a (cm^{-1})
20	1582	(1835) 1861
50	1578	1851
100	1574	1848

The intensity ratio of the two peaks, E_a/E_{2g} , shows typical feature for non-polarized, vertically polarized and parallelly polarized incident beams. As summarized in Table II, the value of ratio E_a/E_{2g} was normalized by one for non-polarized case. It should be noticed that the normalized value strongly depend on the polarization of incident beam and does not depend on the incident power. For vertically polarized incident beam, the normalized ratio becomes larger more than 20%, but it decreases to nearly half for parallelly polarized beam.

Table II Intensity ratio of Raman spectra E_{2g} and E_a for different polarization laser beam

power (mW)	polarization	E_a/E_{2g}	normalized
20	non-polarized	1.29	1.00
	vertical-pol	1.64	1.27
	parallel-pol	0.68	0.53
100	non-polarized	0.55	1.00
	vertical-pol	0.67	1.22
	parallel-pol	0.31	0.56

3.3 Electric properties

Electrical conductivities of individual nanografibers were measured using a micro manipulator by two probe method. The resistance was several $\text{k}\Omega$ per $1\mu\text{m}$, which gives the average conductivity as $1,000\sim 2,000\text{S/cm}$ [8]. Current and voltage characteristics (I - V) were also studied until the dielectric breakdown took place. It was found that the enormously large current density more than 10^7A/cm^2 could flow in a piece of individual nanografibers [6,8].

The temperature dependency (until helium temperature) of electric resistance measured for individual nanografiber showed the both cases metallic and semiconducting [6,8,12]. It should be noticed that there exist the both types of electric resistance in nanografibers.

When these nanografibers were used as field emitters, stable and high emission current was observed [6]. The practically desirable current density 1mA/cm^2 [13] was stably achieved at a fairly low field of $1.2\text{V}/\mu\text{m}$.

3.4 XRD

XRD pattern of mass produced nanografibers is shown in Fig.4. For comparison, XRD of powders prepared from the raw graphite rods (g-powder) also is shown in Fig.4. In XRD patterns of nanografibers strong peaks are observed for 00 l and hk0 reflections.

The peak positions of hk0 reflection are nearly same for nanografibers and g-powder. On the contrary, the peaks of 00 l reflection shift to lower angle side for nanografibers. The graphite layer distance d_{002} ($= c_0/2$) calculated from the peak positions of 002 and 004 reflections, becomes wider from 0.335nm (g-powder) to 0.342nm (nanografibers) [7,14].

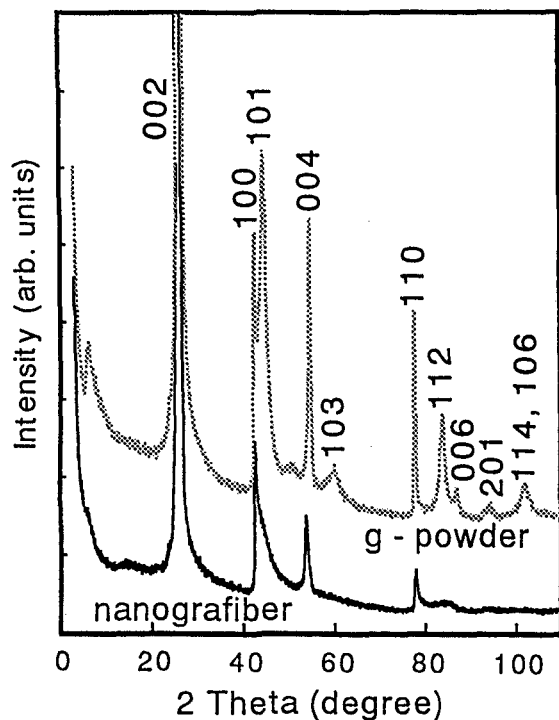


Fig.4 XRD patterns of nanografibers and the raw graphite powder.

4. DISCUSSION AND CONCLUSIONS

In the previous resonance Raman study [11], the breathing modes of nanografibers in the frequency region less than 500 cm^{-1} could be observed similar to the breathing mode in single walled carbon nanotubes [15]. Adding to them, the new Raman peak, E_s , appeared at near 1840 cm^{-1} is characteristic for nanografibers prepared by arc discharge in hydrogen atmosphere [6,7]. The intensity of the Raman peak E_s became stronger at lower pressure of hydrogen gas [6]. In the present study, it was clarified that the intensity of the peak E_s became stronger for vertical polarization incident laser beam, which was vertically polarized to the direction of alignment of nanografibers. This result indicates that the new Raman peak E_s is peculiar to nanografibers and not to nanoparticles or graphite.

Other characteristic features of nanografibers

are electric properties such as high current density and high efficiency of field emission. The difference with graphite is wide layer distance d_{200} as observed in XRD patterns. From the very narrow central channel of nanografibers [6,11] and high graphitization, it is expected that nanografibers have high elastic strength. The mass production of these nanografibers by automatic feed of cathode also is realized.

Acknowledgements

The authors thank Dr. Hiramatsu of Meijo University for allowing use of the facility of Raman spectrometer. This was partially supported by the Grant-in-Aid for Scientific Research on the Priority Area "Fullerenes and nanotubes" by the Ministry of Education, Science and Culture of Japan.

References

- [1] S. Iijima, *Nature*, **354**, 56-58 (1991).
- [2] X. Zhao, M. Ohkohchi, M. Wang, S. Iijima, T. Ichihashi and Y. Ando, *Carbon*, **35**, 775-781 (1997).
- [3] Y. Ando, X. Zhao and M. Ohkohchi, *Carbon*, **35**, 153-158 (1997).
- [4] Y. Saito and S. Uemura, *Carbon*, **38**, 169-182 (2000).
- [5] Y. Ando, X. Zhao and M. Ohkohchi, *Jpn. J. Appl. Phys.*, **37**, L61-L63 (1998).
- [6] Y. Ando, X. Zhao, H. Kataura, Y. Achiba, K. Kaneto, M. Tsuruta, S. Uemura and S. Iijima, *Diamond and Related Materials*, in print.
- [7] X. Zhao and Y. Ando, *Jpn. J. Appl. Phys.*, **37**, 4846-4849 (1998).
- [8] K. Kaneto, M. Tsuruta, G. Sakai, X. Zhao and Y. Ando, *Synthetic Metals*, **103**, 2543-2546 (1999).
- [9] T. W. Ebbesen and P. M. Ajayan, *Nature*, **358**, 220-222 (1992).
- [10] X. Zhao, M. Wang, M. Ohkohchi and Y. Ando, *Jpn. J. Appl. Phys.*, **35**, 4451-4456 (1996).
- [11] H. Kataura, Y. Kumazawa, N. Kojima, Y. Maniwa, I. Umezu, S. Masubuchi et al., *Electronic Properties of Novel Materials --- Science and Technology of Molecular Nanostructures*, Ed. by H. Kuzumany, J. Fink, M. Mehring and S. Roth, American Institute of Physics, (1999) pp.328-332.
- [12] Y. Ando, X. Zhao, H. Shimoyama, G. Sakai, and K. Kaneto, *J. Inorganic Mater.*, **1**, 77-82, (1999).
- [13] Q. H. Wang, T. D. Corrigan, J. Y. Dai, R. P. H. Chang and A. R. Krauss, *Appl. Phys. Lett.*, **70**, 3308-3310 (1997).
- [14] Y. Saito, T. Yoshikawa, S. Bandow, M. Tomita and T. Hayashi, *Phys. Review B*, **48**, 1907-1909 (1993).
- [15] R. Saito, T. Takeya, T. Kimura, G. Dresselhaus and M. S. Dresselhaus, *Phys. Review B*, **57**, 4145-4153 (1998).